Journal of Industrial Microbiology (1995) 15, 176–185

Adhesin receptors of human oral bacteria and modeling of putative adhesin-binding domains

FJ Cassels[1], CV Hughes[2] and JL Nauss[3]

[1]*Department of Gastroenterology, Division of Medicine, Walter Reed Army Institute of Research, Washington, DC 20307-5100;* [2]*Department of Pediatric Dentistry, Boston University, Boston, MA, 02118-2392;* [3]*Department of Chemistry, University of Cincinnati, Cincinnati, OH, 45221-0172, USA*

Adherence by bacteria to a surface is critical to their survival in the human oral cavity. Many types of molecules are present in the saliva and serous exudates that form the acquired pellicle, a coating on the tooth surface, and serve as receptor molecules for adherent bacteria. The primary colonizing bacteria utilize adhesins to adhere to specific pellicle receptor molecules, then may adhere to other primary colonizers via adhesins, or may present receptor molecules to be utilized by secondary colonizing species. The most common primary colonizing bacteria are streptococci, and six streptococcal cell wall polysaccharide receptor molecules have been structurally characterized. A comparison of the putative adhesin disaccharide-binding regions of the six polysaccharides suggests three groups. A representative of each group was modeled in molecular dynamics simulations. In each case it was found that a loop formed between the galactofuranoseβ (Gal$f\beta$) and an oxygen of the nearest phosphate group on the reducing side of the Gal$f\beta$, that this loop was stabilized by hydrogen bonds, and that within each loop resides the putative disaccharide-binding domain.

Keywords: adhesin receptors; streptococcal polysaccharides; coaggregation; salivary proteins; molecular modeling

Introduction

The human mouth contains several diverse microbial habitats. The enamel surface of the tooth crown, the epithelial tissues of the oral mucosa and gingiva and the cementum of the dental root surface offer a variety of sites for bacterial adherence. These sites are continually bathed and coated with saliva and serous exudates from the gingival crevice. Proteins, glycoproteins, and mucins contained in these fluids, cell-bound glycoproteins and glycolipids, and extracellular matrix proteins provide a great diversity of possible receptor molecules for microbial recognition and have all been found to serve as receptor molecules for microbial adherence proteins (adhesins). A result of the many available habitats and characteristics of adherent receptor molecules is a form of tissue tropism with specific bacteria characteristically found in each ecological niche. The mucosal surfaces are characterized by rapid cell turnover with continuous desquamation of the superficial epithelial cells and microbial flora. In contrast, the hard nonshedding surfaces of the teeth have the potential for the formation of thick microbial biofilms known as dental plaque. After a thorough cleaning of the tooth surface, the tooth is rapidly coated, primarily with salivary proteins, but also with host and bacterial cellular debris. This coating, termed the acquired pellicle, serves as a substratum for the primary (early) colonizing species of bacteria. The surfaces of these bacteria add yet another possibility of receptors for additional bacterial colonization. This cell-to-cell recognition between genetically distinct bacterial types, termed coaggregation, appears to be important in the accretion of dental plaque [52]. Coaggregation interactions can be intrageneric, intergeneric, or multigeneric, and most coaggregation interactions are inhibitable by simple sugars [52]. The primary colonizing species in dental plaque are mostly Gram-positive species, and the secondary (later) colonizing species mostly Gram-negative. Of the primary colonizers, streptococci predominate. *Streptococcus oralis*, *S. sanguis* and *S. mitis* account for 80% of primary colonizers, with *Actinomyces naeslundii* (including formerly *A. viscosus* strains) accounting for an additional 10% [69]. The streptococci appear to be well suited to function as primary colonizers as multiple adherence strategies have been characterized, which may in large part account for their success in colonization. The uniqueness and diversity of surfaces in the oral cavity create and result in diverse bacterial habitats in the mouth and are thus reflected in the complexity of the bacterial flora found there.

This review focuses on the receptor aspects of oral microbial adherence, initially describing several types of receptor molecules, then discussing the group of streptococcal receptor molecules that as a group have been well characterized. This group consists of the cell–wall polysaccharide coaggregation receptors of *S. oralis* ATCC 55229, *S. oralis* 34, *S. oralis* C104, *S. gordonii* 38, *S. oralis* J22, and *S. oralis* ATCC 10557 [52,78]. Structural and func-

Correspondence: FJ Cassels, Department of Gastroenterology, Division of Medicine, Walter Reed Army Institute of Research, Washington, DC 20307-5100, USA

Abbreviations used are as follows: *f*, furanose; Fuc, D-fucose; Gal, D-galactose; GalNAc, *N*-Acetyl-D-Galactosamine; Glc, D-glucose; Glyc, glycerol; HPLC, high-performance liquid chromatography; HPTLC, high-performance thin-layer chromatography; HF, hydrofluoric acid; LacCer, lactosyl ceramide; NeuAc, *N*-Acetyl neuraminic acid; NMR, nuclear magnetic resonance; PRG, proline-rich glycoproteins; PRP, proline-rich proteins; *p*, pyranose; Rha, L-rhamnose; RMSD, root-mean-square differences

Received 30 December 1994; accepted 14 June 1994

tional aspects of the receptor molecules will be discussed. Structural differences result in the grouping of these six receptors into three groups based on the structure of the putative adhesin-binding domains. Included in the analysis of the three groups of streptococcal receptor molecules are preliminary results of molecular modeling of the receptors. Results indicate that hydrogen bonding between the common β-galactofuranose (Galfβ) residue and the phosphate residue at the reducing end of the Galfβ allows a loop to form and subsequently stabilize the putative disaccharide adhesin-binding domain within the loop.

Receptors for oral bacteria

The microbial ecology of the mouth and the contributions that adherence plays in it have been the subject of considerable research over the last several decades. The vast majority of reports on this research describe the adherence properties of oral bacterial isolates and their putative roles in colonization of the mouth. Less numerous are papers that definitively identify and characterize adhesive molecules which mediate attachment to oral surfaces. Both the adherence properties of oral bacterial isolates and their adhesins have been the subject of other reviews [52,53] and will not be the focus of this paper. Another active area of investigation, although perhaps less so than the previously mentioned ones, is the identification and characterization of receptors for bacterial adhesins on oral epithelial cells, in saliva, on enamel and other dental tissues and on other bacteria. In recent years a number of investigators have begun to identify and characterize some of these receptors. Understanding how these receptors function during oral bacterial colonization and dental plaque formation may have important implications in understanding the microbial ecology of the mouth and the pathogenesis of oral bacterial diseases. While a complete review of the literature which has contributed to our knowledge of receptors for oral bacterial adhesion is beyond the scope of this review, a representative portion of data regarding receptors for oral bacterial adherence is provided in Table 1.

Most of the research in this area has focused on salivary molecules. Saliva coats most surfaces in the mouth, including bacteria found there, and it is perhaps not surprising that many oral bacteria possess mechanisms to recognize specific salivary molecules. The recognition of salivary molecules in their soluble forms leads to the phenomenon of agglutination. Agglutination was initially recognized by the observation that saliva agglutinates whole cells of many oral bacterial isolates. This property of certain salivary molecules has been proposed alternatively to function as a mechanism for bacterial clearance in the mouth and as an aid to bacterial colonization. Several groups have identified molecules from saliva which act as agglutinins. Ericson and Rundegren [30] identified a large ($MW > 5 \times 10^6$) agglutinin from parotid saliva. Similarly, Levine *et al* [61] identified a large glycoprotein from submandibular saliva with agglutinating activity. In both cases, the carbohydrate composition of each molecule was greater than 40% and with high fucose and hexose content with a relatively low amount of sialic acid. Interestingly, the agglutination of a *S. sanguis* strain reported by Levine *et al* [61] is inactivated by neuraminidase treatment while the agglutination of *S. mutans* is resistant to neuraminidase treatment. In contrast, Babu *et al* [7] identified a 60-kDa glycoprotein with agglutinating activity from saliva which apparently involved recognition of the polypeptide portion of the molecule. The agglutinating activity was unaffected by deglycosylation of the molecule. Demuth *et al* [24–26] recently identified, purified, and cloned bacterial adhesins from both *S. sanguis* and *S. mutans* which recognize an agglutinin from parotid saliva.

More recently, specific receptors for oral bacterial adherence in saliva have been identified with assays that utilize saliva or salivary molecules bound to solid surfaces. The saliva-coated hydroxyapatite assay, originally designed for characterizing bacterial adherence to the tooth surface, has been used to identify specific salivary components which mediate bacterial binding. Using this assay, Gibbons and Hay [32] have elegantly identified salivary components which mediate binding of *A. naeslundii* (*viscosus*) to saliva-coated hydroxyapatite. They demonstrated that *A. naeslundii* (*viscosus*) LY7 bound preferentially to hydroxyapatite beads coated with the acidic proline-rich proteins and statherin of human saliva. The acidic proline-rich proteins (PRP) have been identified in human and other primate salivas [72,73]. PRP-1, PRP-2 and PIF-slow (PIF designates an isoform of PRP) are 150-amino acid polypeptides which differ in that residues 4 and 50 are asparagine and aspartate (PIF-slow), aspartate and asparagine (PRP-1) or both aspartate (PRP-2). Three other PRPs (PIF-fast, PRP-3, PRP-4) are 106-amino acid polypeptides corresponding to the first 106 residues from the larger PRPs [44]. Gibbons and Hay demonstrated that smaller concentrations of the larger PRPs were required to promote maximal bacterial binding. Thus, it appears that the 44-amino acid terminus enhanced but was not essential to binding. Perhaps the most significant finding of these studies was the observation that PRP-1 in its soluble form did not bind to *A. naeslundii* (*viscosus*). Thus it appeared that epitopes recognized by the bacteria were not exposed in the molecule's soluble form. This proposal is supported by studies of the calcium-binding properties of the molecules and thermodynamic studies of their adsorption to hydroxyapatite which suggested that PRPs undergo a major conformational change when they adsorb to hydroxyapatite [10,67]. Thus, it appears *A. naeslundii* (*viscosus*) is capable of distinguishing between soluble and bound PRPs.

Additional evidence of the remarkable specificity of receptor recognition by oral bacteria has been provided by Fisher and colleagues. Using a technique that separates proteins in saliva by SDS polyacrylamide gels and then transfers them to nitrocellulose membrane [76], receptors in saliva for *Fusobacterium nucleatum* and oral *Streptococcus* spp have been identified [37,68,77]. Using this technique they demonstrated that *F. nucleatum* bound to a 89-kD glycoprotein. Subsequently they showed that deglycosylation of the protein resulted in the loss of receptor activity. Amino acid analysis showed it to be a member of the class of human salivary proteins known as proline-rich glycoproteins (PRG) [37]. To characterize the receptor activity of the carbohydrate portion of the glycoproteins they first analyzed PRG oligosaccharides by a combination of mass

Table 1 Receptors for oral bacterial adhesins identified as host salivary proteins, as other bacterial components, as glycolipids, and as host extracellular matrix components

Receptor (fine specificity)	Adherent species[a] strain (ligand)	Detection of adherence	Ref
Host salivary proteins			
agglutinin	*S. mutans* serotype c	agglutination	[30]
agglutinin	*S. sanguis*	agglutination	[24]
α-amylase	*S. sanguis*	parotid saliva/overlay	[27,81]
mucin	*S. sanguis*	glass	[83]
mucin	*S. sanguis*	overlay assay	[68]
PRG-1[b](Galβ1→4GlcNAc)	*F. nucleatum*	saliva	[37,77]
PRG	*S. sanguis*	overlay assay	[68]
PRG	*S. sanguis* G9B	agglutination	[11]
PRG	*A. naeslundii* T14V[c] (Type 1 fimbriae)	latex bead aggregation	[35]
acidic PRP-1[d]	*A. naeslundii* T14V (Type 1 fimbriae)	latex bead aggregation	[21,35]
acidic PRP	*A. naeslundii* LY7[c]	parotid saliva/SHA[e]	[32]
acidic PRP	*P. gingivalis* (fimbrillin)	parotid saliva/SHA	[5]
acidic PRP (Pro-Gln)	*S. gordonii*	saliva/SHA	[36]
acidic PRP	*S. mutans* JBP	saliva/SHA	[34]
basic PRP	*A. naeslundii* T14V (Type 1 fimbriae)	latex bead aggregation	[21]
statherin	*P. gingivalis* (fimbrillin)	parotid saliva/SHA	[5]
statherin	*A. naeslundii* LY7	parotid saliva/SHA	[32]
60-kD glycoprotein	*S. mutans*	agglutination	[7]
160-kD protein	*A. naeslundii*	KB epithelial cells	[12]
180-kD protein	*A. naeslundii*	saliva/buccal epithelial	[8]
300-kD protein	*S. mutans* serotype c	saliva/SHA	[49,50]
Bacterial components			
S. oralis ATCC 55229 PS[f] (Rhaβ1→2Rha)	*C. ochracea* ATCC 33596 (155-kD protein)	coaggregation	[15,16,39] [52,91]
S. oralis 34 PS (GalNAcβ1→3Gal)	*A. naeslundii* T14V and *A. naeslundii*	coaggregation	[64,66]
S. oralis C104 PS (GalNAcβ1→3Gal)	*A. naeslundii*	coaggregation	[4]
S. gordonii 38 PS (GalNAcβ1→3Gal)	*A. naeslundii* T14V and *A. naeslundii*	coaggregation	[78]
S. oralis J22 PS (Galβ1→3GalNAc)	*A. naeslundii* T14V and *A. naeslundii*	coaggregation	[2]
S. oralis ATCC 10557 PS (Galβ1→3GalNAc)	*A. naeslundii* T14V and *A. naeslundii*	coaggregation	[3]
F. nucleatum protein	*Streptococcus* spp	coaggregation	[48]
glucan	*S. cricetus*	aggregation	[28]
glucan	*S. gordonii*	saliva/SHA	[45]
glucan	*S. mutans*	saliva/SHA	[82]
glucan	*S. sobrinus*	saliva/SHA	[33]
Glycolipids[g]			
GM1 (Galβ3GalNAc)	*A. naeslundii* ATCC 12104	TLC[h]/overlay	[14]
GD1b (Galβ3GalNAc)	*A. naeslundii* ATCC 12104	TLC/overlay	[14]
globoside (Galβ3GalNAc)	*A. naeslundii* ATCC 12104	TLC/overlay	[14]
Gb3b (GalNAcβ)	*A. naeslundii* ATCC 12104 *A. naeslundii* ATCC 19246[c]	TLC/overlay	[85]
GgO3 (GalNAcβ)	*A. naeslundii* ATCC 12104 *A. naeslundii* ATCC 19246	TLC/overlay	[85]
Gb4a (Galβ)	*A. naeslundii* ATCC 12104	TLC/overlay	[85]
GgO4 (GalNAcβ)	*A. naeslundii* ATCC 12104 *A. naeslundii* ATCC 19246	TLC/overlay	[85]
LacCer (Galβ1→4Glc)	*A. naeslundii* ATCC 12104	TLC/overlay	[85]
LacCer (Galβ1→4Glc)	*A. naeslundii* ATCC 19246	TLC/overlay	[85]
Host extracellular matrix			
collagen Type I	*A. naeslundii* LY7	hydroxyapatite assay	[63]
collagen Type I	*S. mutans*	soluble	[88]
collagen Type I	*S. rattus*	saliva/SHA	[62]
collagen Type III	*A. naeslundii* LY7	hydroxyapatite assay	[63]
collagen Type V	*S. cricetus*	saliva/SHA	[62]
fibrinogen	*A. naeslundii*	hydroxyapatite assay	[43]
fibrinogen	*B. intermedius*	radioassay	[56,60]
fibrinogen	*P. gingivalis*	radioassay	[56,58,59]
fibrinonectin	*P. gingivalis*	radioassay	[57]

[a]*S, Streptococcus; F, Fusobacterium; A, Actinomyces; P, Prevotella; B, Bacteroides; C, Capnocytophaga*
[b]PRG, proline-rich glycoprotein; [c]Formerly *A. viscosus*; [d]PRP, proline-rich protein
[e]SHA, saliva-coated hydroxyapatite
[f]PS, cell-wall polysaccharide
[g]GM1, Galβ1→3GalNAc1→4(NeuAcα2→3)Galβ1→4Glc→Ceramide (Cer); GD1b, Galβ1→4GalNAcβ1→4(NeuAc2→8NeuAc2→3)Galβ1→4Glc→Cer; globoside, GalNAcβ1→3Galα1→4Galβ1→4Glc→Cer; Gb3b, Galα1→3Galβ1→4Glc→Cer; GgO3, GalNAcβGalβ1→4Glc→Cer; Gb4a,GalNAcβ1→3Galα1→4Galβ1→4Glc→Cer; GgO4, Galβ1→3GalNAcβ1→4Galβ1→4Glc→Cer; LacCer, Galβ1→4Glc→Cer
[h]TLC, thin-layer chromatography

spectrometry and nuclear magnetic resonance spectroscopy. They identified 27 different highly fucosylated structures. The major structure is a biantennary asialosaccharide that contains two fucose residues on one antenna. The other antenna contains an unsubstituted terminal lactosamine. By screening *F. nucleatum* binding to glycolipids and neoglycolipids carrying carbohydrate structures related to those of the PRG, they were able to characterize the fine specificity of the *F. nucleatum* recognition. By analysis of the binding of *F. nucleatum* to these model compounds, they demonstrated that the bacterium bound structures which contain unsubstituted Galβ1→4GlcNac residues. Addition of *N*-acetyl neuraminic acid (NeuAc) or L-fucose (Fuc) to the residues prevented adherence. These observations suggested that the major structure they detected could act as a bacterial receptor at its unsubstituted terminal lactosamine. Interestingly, the studies also demonstrated that *F. nucleatum* could recognize terminal Galβ1→3GalNAc residues, a disaccharide not found on the PRG glycoprotein. Subsequent studies demonstrated that saliva from individuals that lack proline-rich glycoprotein G1 fails to interact with *F. nucleatum* [6].

A similar approach has enabled investigators to characterize possible receptors for actinomyces in the oral cavity. *Actinomyces* spp, a prominent member of the oral flora, have been shown to express two antigenically distinct fimbrial types [18,20]. Type 2 fimbriae are associated with a lactose-sensitive binding to oral streptococci, agglutination of human erythrocytes and binding to epithelial cells [13,23,55]. Type 1 fimbriae are thought to mediate binding to the saliva-coated tooth surface discussed above [21,22,35]. The different adhesive properties of the two types of fimbriae and their distribution on fresh oral isolates suggests that the expression of these two distinct fimbriae is of ecological significance. Earlier inhibition studies with soluble saccharides and an overlay technique characterized the specificity of the type 2 fimbriae for terminal Galβ residues [12,65]. Analysis of the fimbrial adhesins from *A. naeslundii* ATCC 12104 (formerly WVU45) and *A. naeslundii* (formerly *viscosus*) T14V demonstrated that sialidase-treated KB epithelial cells were best inhibited with plant lectins specific for GalNAc and Galβ1→3GalNAc [18]. The glycolipid binding specificities of *A. naeslundii* ATCC 12104 (WVU45) demonstrated that Galβ1→3GalNAc present on gangliosides and the GalNAcβ1→3Gal terminus of globoside could both serve as receptors for this lectin [14]. A subsequent analysis of *Actinomyces* binding by Strömberg and Karlsson characterized two distinct specificities [85]. The first, demonstrated by strains of both *A. naeslundii* 12104 and *A. naeslundii* (*viscosus*) 19246 was a low affinity binding to lactosylceramide (LacCer). Interestingly, the activity of free LacCer was dependent on the ceramide structure; species with 2-hydroxy fatty acid and/or a trihydroxy base were positive while those with nonhydroxy fatty acids and a dihydroxy base were negative. The binding characteristics for LacCer were nearly identical for *A. naeslundii* 12104 and *A. naeslundii* (*viscosus*) 19246. They were also very similar to those seen for *Propionibacterium granulosum* in a related study [86]. The second binding specificity identified was for terminal or internal GalNAcβ exhibited by the adhesin from *A. naeslundii* 12104. This binding was felt to be equivalent to the galactose- and lactose-inhibitable specificity described by previous studies. Moreover, they suggested that terminal Galβ structures on several glycolipids were not recognized by these strains. Further studies of actinomyces isolates demonstrated strain differences in fine specificity for GalNAcβ containing receptors as evidenced by the number of cells bound to glycosphingolipids and the effect of neighboring sugar groups on binding [84]. Interestingly, they also showed functional differences in binding between the two strains. *A. naeslundii* (*viscosus*) LY7 bound in higher numbers to buccal epithelial cells while strain ATCC 12104 alone showed GalNAcβ sensitive saliva aggregation. Mucosal isolates of *Actinomyces* more often showed LY7-like specificities while those isolated from dental plaque resembled strain ATCC 12104. Thus, it appears that these differences in specificities may be reflected in differences in colonization patterns of the organism.

In addition to interacting with receptors in saliva and on epithelial cells and teeth, oral bacteria also interact with molecules found in the host extracellular matrix (Table 1). Binding specificities for collagen, fibronectin, and fibrinogen have been described for a variety of oral bacterial species. Lantz and colleagues demonstrated that a number of the bacterial surface components that recognize these molecules may also have enzymatic activities that degrade them [56–59]. This coupling of recognition and degradation may play a role in mediating virulence of the putative periodontal pathogen *Porphyromonas gingivalis*.

Streptococcal adhesin coaggregation receptors

Of the bacterial components utilized as receptor molecules listed in Table 1, the streptococcal adhesin coaggregation receptors have recently drawn considerable attention. While the adhesin receptors are one mechanism by which streptococci participate in coaggregation reactions, initial adherence occurs through the use of adhesin molecules that bind to pellicle [31], or to primary colonizing species [54]. In a classic paper in the coaggregation literature, Cisar *et al* [19] studied the coaggregation interactions between 26 streptococcal strains and 26 actinomyces strains in terms of which streptococcal strains coaggregated with which actinomyces strains. As a result, the streptococci fell into four groups and the actinomyces into two groups based on whether coaggregation was lactose-inhibitable, and whether heating of one or both partners blocked subsequent coaggregation. *S. oralis* ATCC 55229 (formerly *S. sanguis* strain H1) fell into group 2 based on the lack of coaggregation after *S. oralis* ATCC 55229 was heated, and because the coaggregation was not lactose-inhibitable. This indicated that in both actinomyces groups A and B interactions, *S. oralis* ATCC 55229 utilized adhesins to coaggregate (not receptor molecules). *S. gordonii* 38, *S. oralis* 34 and *S. oralis* C104 all fell into group 3 based on lactose-inhibitable coaggregation that was abolished on heating of the actinomyces strain (adhesin molecule was present on only the groups A and B actinomyces). *S. oralis* J22 fell into group 4 based on the necessity of heating both partner cells to abolish coaggregation (adhesin and receptor molecules present on

both partner cells), and because the coaggregation was not inhibited by lactose. This study [19] was recently revisited [47], with additional strains added as well as additional characteristics examined, ie hemagglutination properties and aggregation of PRP-coated latex beads. In addition, *S. oralis* ATCC 10557 was examined and found to be a member of group 3.

S. oralis ATCC 55229 was further investigated by Weiss *et al* [92] demonstrating that *C. ochracea* ATCC 33596 possessed an adhesin molecule for receptors on *S. oralis* ATCC 55229, *A. naeslundii* PK984 and *A. israelii* PK16, that these interactions were inhibited by Rha, Fuc and to a lesser extent by β-methylgalactoside and lactose, and that the adhesin molecule was a non-fimbrial outer membrane protein of 155 kD [91]. Cassels and London [16] isolated the cell–wall coaggregation-inhibiting polysaccharide for the *C. ochracea* ATCC 33596 interaction, and they structurally characterized the hexasaccharide repeating unit [15], and the intact polysaccharide (structure given in Figure 1) [39]. A coaggregation-defective mutant of *S. oralis* ATCC 55229 did not contain the hexasaccharide repeating unit or polysaccharide [16]. For details on the purification and characterization of these streptococcal polysaccharide molecules refer to Cassels and van Halbeek [17] and Abegunawardana and Bush [1].

The first coaggregation-inhibiting polysaccharide studied was that of *S. oralis* 34, in streptococcal group 3. McIntire *et al* [64,66] purified and characterized this molecule (Figure 1). The coaggregation of *S. oralis* 34 with *A. naeslundii* T14V was inhibitied most effectively by GalNAcβ- and Galβ-containing saccharides [18,66]. After the structural characterization of the *S. oralis* 34 repeating unit, the disaccharide containing the GalNAcβ was designated as the receptor-binding domain [64]. Polysaccharides from three other group 3 members, *S. oralis* strains ATCC 10557, C104, and *S. gordonii* 38 have been purified and structurally characterized [3,4,78]. *S oralis* C104 and *S. gordonii* 38 also contained the GalNAcβ1→3Gal disaccharide, the putative adhesin-binding domain, while *S. oralis* strains ATCC 10557 and J22 (Figure 1) both possess the structure Galβ1→3GalNAc [2]. Earlier analysis of the adhesin-binding specificities of actinomyces was presented above. The overall conclusion from this series of studies is that the lectin-combining site in these *Actinomyces* strains are able to bind to either of the two putative binding domains with approximately equal binding affinities.

The putative adhesin-binding domain of *S. oralis* ATCC 55229 is the disaccharide Rhaβ1→2Rha [52], a unique feature of *S. oralis* ATCC 55229 not present in any of the streptococcal polysaccharides characterized to date. The other five polysaccharides characterized are different from those of *S. oralis* ATCC 55229, but among themselves have similar binding and inhibition profiles, ie *Actinomyces* adhesin binding, inhibition by GalNAc and Galβ1→3GalNAc specific plant lectins, and by glycolipid binding profiles. Hsu *et al* [47] in contrast suggest that GalNAc-sensitive adhesins of certain streptococcal species specifically recognize streptococci with GalNAcβ1→3Gal containing polysaccharides. Although binding and inhibition data of the actinomyces-streptococcal interactions are similar, the structure of the putative adhesin-binding domains differ. As seen in Table 1, *S. oralis* strains 34, and C104 and *S. gordonii* 38 fall into the GalNAcβ1→3Gal group possessing the putative receptor-binding domain, while *S. oralis* strains J22 and ATCC 10557 fall into the Galβ1→3GalNAc group. Of additional interest is a report on the structural characterization of *S. mitis* K103 cell wall polysaccharide [79]. This strain of streptococci does not fall into any coaggregation group due to its lack of coaggregation with actinomyces, lack of hemagglutination or lack of PRP/latex bead agglutination properties [47]. While superficially similar to the other streptococcal polysaccharides shown in Table 1, no Gal*f*β residue is present, and none of the putative adhesin-binding sites is present in the *S. mitis* K103 structure.

Our objectives were several fold: 1) to compare the primary structures of the six streptococcal polysaccharide receptor molecules and group by structural similarities, 2) model by molecular dynamics simulations a representative of each group of receptors, and 3) compare the molecular

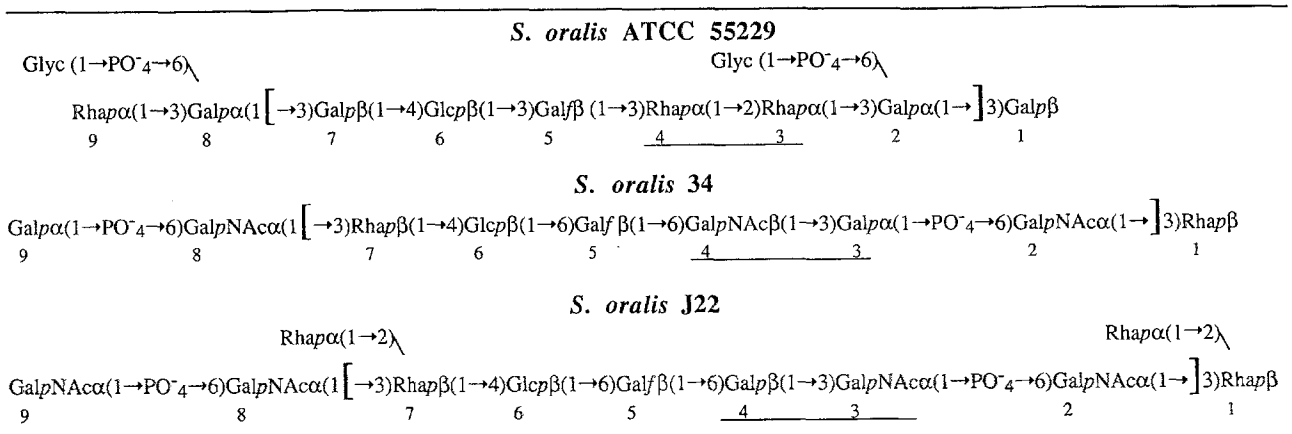

Figure 1 Structures of the three *Streptococcus oralis* adhesin receptor carbohydrate sequences modeled. Abbreviations: Rha, L-Rhamnose; Gal, D-Galactose; Glc, D-Glucose; GalNAc, *N*-Acetyl-D-Galactosamine; Glyc, Glycerol; *p*, pyranose; *f*, furanose. Square brackets denote repeating hexasaccharide (*S. oralis* strains ATCC 55229 and 34) or heptasaccharide (*S. oralis* J22) unit depicted in Figure 2. Individual monosaccharides in the main chain are numbered from the reducing end and discussed in the text; the underlined region indicates the putative adhesin-binding domain

models derived from the different groups for similarities and differences.

Molecular modeling methodology

Molecular modeling was conducted on a Silicon Graphics 4D/35 Personal Iris using the software packages InsightII (version 2.3.5) and Discover (version 2.9.5), both from Biosym Technologies, San Diego, CA, USA. The forcefield used was the AMBER forcefield [90] as implemented by Biosym with the extensions for polysaccharides developed by Homans [46]. All calculations were performed *in vacuo* with a distance-related dielectric constant. The absence of solvent is considered acceptable as this study is a search for possible conformations of the oligosaccharides. Thus, the goal was to sample as wide an area of conformational space as possible. Similar studies *in vacuo* have been performed with other carbohydrate molecules [9,41]. Inclusion of solvent has been found to have little effect of conformational transitions but will dampen torsion angle fluctuations [9,29,42,46].

Models were built of *S. oralis* ATCC 55229 (representing the Rhaβ1→2Rha putative adhesin-binding domain group), *S. oralis* 34 (representing the GalNAcβ1→3Gal putative adhesin-binding domain group), and *S. oralis* J22 (representing the Galβ1→3GalNAc putative adhesin-binding domain group) carbohydrate receptors using the InsightII Biopolymer module and the default glycosidic torsion angles and ring conformations. The sequences for each oligosaccharide were taken from Kolenbrander *et al* [52] and are given in Figure 1. Each model consisted of nine main chain sugar residues. The galactofuranose residues were positioned in the middle of the segment to be studied (residue 5, Figure 1). The lengths of the models were chosen to have approximately equal numbers of sugar residues on either side of the Gal*f*β and to include a phosphodiester residue on either side. Initially, each model was subjected to an energy minimization procedure. Nonbonded calculations were cut off at 15.0 Å with a switching potential for 1.5 Å. Minimization was carried out until the maximum energy derivative was less than 1.0 kcal $Å^{-1}$. In all cases, the final minimized structure did not vary significantly from the starting structure. Each minimized structure was then subjected to a brief molecular dynamics simulation at either 300 or 900 K. After an initialization period of 1000 steps, the simulation was conducted for 50 000 steps with every 100 steps being saved for a total of 511 frames. The step size was 1.0 femtoseconds. The resulting trajectory was analyzed via a cluster analysis based on the root-mean-square differences (RMSD) between all saved structures within a run. The trajectories were then broken into three to six groups of families based on the RMSD. A representative for each family was selected as the average coordinates of all structures within the family. Each representative structure was further subjected to an energy minimization procedure as described earlier. The resulting lowest energy representative structure within any single molecular dynamics trajectory was then selected for further analysis. In all analyses, hydrogen bonds were identified using the InsightII default definitions. The molecular dynamics simulation results presented are preliminary with longer simulations, some including solvent, and a more thorough analysis of the trajectories currently underway. This information and more detailed descriptions of methodology used will be included in a forthcoming report.

Molecular modeling results

In all cases, the model oligosaccharide chains folded in upon themselves at some point in the simulation. The galactofuranose residues were particularly flexible throughout the trajectories in agreement with previous studies concerning the flexibility of furanose rings [70,71,89]. All trajectories at either 300 or 900 K were well-behaved and stabilized early in the runs.

The simulation with the *S. oralis* ATCC 55229 model reached equilibrium near frame 125 as determined by the total and potential energies during the course of the simulation. Concurrent with the stabilization of the energy of the system was the formation of two particularly stable hydrogen bonds between one of the phosphate oxygens attached to the α-D-galactopyranose (residue 2, see Figure 1) and two hydroxyl groups of the galactofuranose (residue 5) (Figure 2A). The first hydrogen bond to the C5 hydroxyl group appears at approximately step 80 and essentially remains intact throughout the simulation. The second hydrogen bond to the C2 hydroxyl group appears shortly afterwards near step 130 and also remains present to the conclusion of the simulation. These hydrogen bonds help stabilize a loop formed in the sequence Gal*f*β(1→3)Rha*p*α(1→2)Rha*p*α(1→3)(Glyc(1→PO_4^-→6))Gal*p*α. The formation of the loop is probably enhanced by the rhamnosyl 1→2 and 1→3 linkages. As a result of the loop formation, the methyl groups from the rhamnose residues are protruding away from the loop and are clearly exposed thus providing unique hydrophobic contact points for the coaggregation partner cell adhesin.

The molecular dynamics simulation at 300 K for the *S. oralis* 34 model appeared to fall into a local minimum. The ends of the oligomer folded in with several interactions between the ninth residue (Galα), the neighboring phosphate, and the penultimate sugar residue of the model (GalNAcα). The total and potential energies for the system dropped approximately 100 kcal mol^{-1} in the first 75 frames and remained steady for the remainder of the simulation. The ends of the oligomer came together near enough for hydrogen bond interactions within 75 frames and remained so for the duration of the run. To take a wider sampling of the conformational space for the *S. oralis* 34 model, a separate simulation at 900 K was performed. The model in this simulation was considerably more flexible. More significantly, a loop formed from residues 5 to 3 (Gal*f*β(1→6)Gal*p*NAcβ(1→3)Gal*p*α(1–PO_4^-). The loop was stabilized by a hydrogen bond between one of the phosphate oxygens and the C2 hydroxyl group of the galactofuranose, a similar type of interaction as observed in the models of *S. oralis* ATCC 55229 and J22 (discussed below) at 300 K. This interaction is only present for approximately 110 frames, the vast majority at the end of the simulation. As a result of the loop, the *N*-acetyl group on residue four is completely exposed to the solvent and could serve as an important feature of specific recognition (Figure 2B).

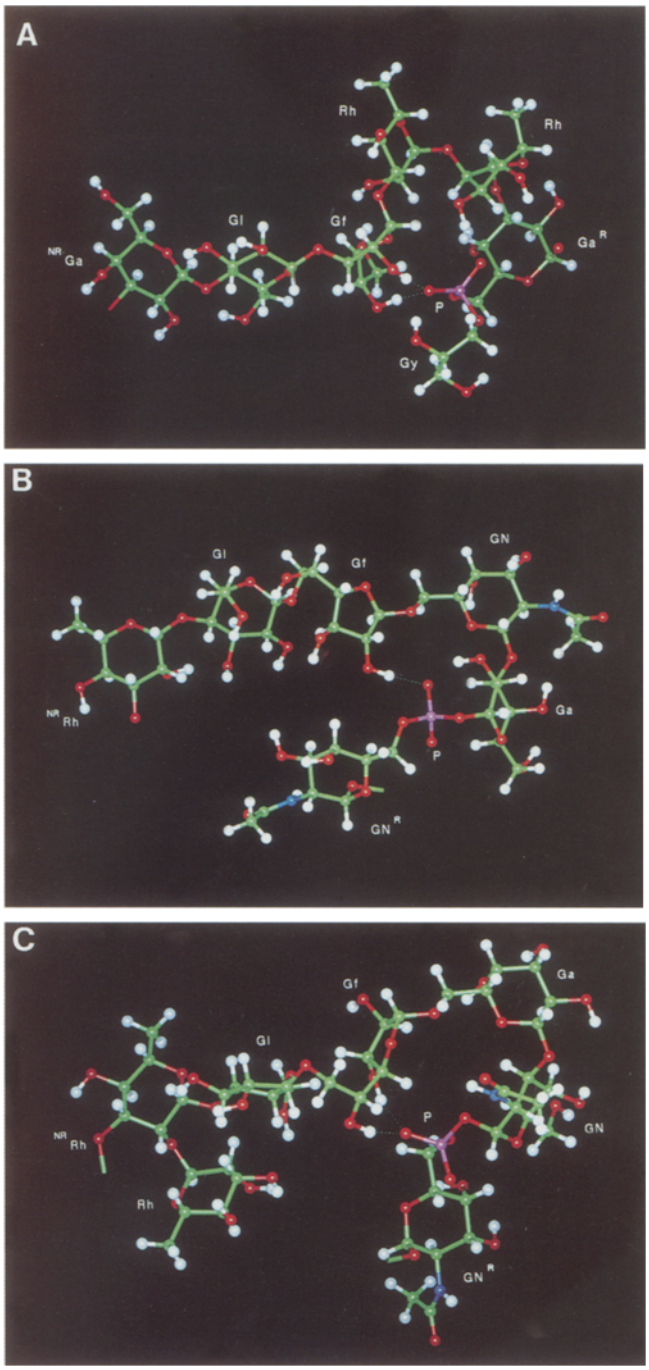

Figure 2 A molecular model of the repeating unit portion of the *Streptococcus oralis* adhesin polysaccharide receptor. See Figure 1 for the complete structure utilized in calculations. (A) *S. oralis* ATCC 55229. (B) *S. oralis* 34. (C) *S. oralis* J22. Abbreviations: Rh, Rhamnopyranose; Ga, Galactopyranose; Gl, Glucopyranose; GN, *N*-Acetyl-Galactopyranosamine; Gf, Galactofuranose; P, Phosphate; Gy, Glycerol; NR, Non-reducing terminus; R, Reducing terminus. Atom color code: White, hydrogen; Red, oxygen; Green, carbon; Blue, nitrogen, Magenta; phosphate. Dotted lines indicate hydrogen bonding interactions

The simulation for the *S. oralis* J22 carbohydrate receptor showed it to be a very flexible molecule. None of the clusters greatly resembled each other and the model went through several cycles of extension and contraction as defined by the oligomer end-to-end distances. Again, the Gal*fβ* residue played an important role in the flexibility of the model, and in this specific situation, even more so than with the *S. oralis* ATCC 55229 model. The Glcβ (residue 6) is linked to the Gal*fβ* at C6 thus having four exocyclic bonds to rotate. Despite the mobility displayed by this model, the total and potential energies for the trajectory were stable. Equilibrium was reached quickly within the first 50 steps. The lowest energy family representative for this trajectory appeared between frames 300 and 400. During this time, the end-to-end distance shrank from a maximum of 28 Å to the minimum observed of 6 Å. Also, two hydrogen bonds were formed between the intrachain phosphate lying between residues three and two (Gal*p*NAcα(1→PO^-_4→6)Gal*p*NAcα) and the preceding Gal*fβ* (residue five) (Figure 2C). Each of these two hydrogen bonds has an oxygen of the phosphate as an acceptor and has donor groups as the C3 and C5 hydroxyl groups. The interaction between the phosphate and the C5 Gal*fβ* group is the longer lasting of the two, remaining intact for most of the remainder of the simulation. The hydrogen bond to the C3 hydroxyl group is lost after frame 417.

The result of these interactions is a loop encompassing the region of Gal*fβ*(1→6)Gal*p*β(1→3)Gal*p*NAcα(1→PO^-_4). This loop is very similar to that found in the *S. oralis* ATCC 55229 model albeit smaller. There are only two sugar residues between the Gal*fβ* and the phosphate in the *S. oralis* J22 model as opposed to three in the *S. oralis* ATCC 55229 model. However, the loop is made complete in both cases by hydrogen bonds between the phosphate and either a ring or C5 hydroxyl group in the Gal*fβ*. This loop exposes to the solvent two possible specific recognition sites for the adhesin: the complete Galβ residue and the *N*-acetyl group on the adjacent galactose.

Molecular modeling discussion

A common folding motif clearly was found at or near each putative adhesin-binding site modeled. A loop is formed consisting of three or four sugar residues plus the nearest phosphate to the reducing end. This loop is held together at the base by hydrogen bonding interactions between the phosphate and the Gal*fβ* residue. The loops are further characterized by having one member of the ring as either a Rha or a GalNAc. Formation of the loop is enhanced by the presence of 1→3 glycosidic linkages which predispose the sequence to form a turn. No similar type of loop structure appears to have been reported for any other oligosaccharides. In addition, this report appears to be the first modeling study of an oligosaccharide containing phosphate. Another molecular dynamics simulation of a carbohydrate ligand reported is that of an asialoglycoprotein receptor ligand [9].

The i to i+3 or i+4 hydrogen bonds observed in this study are not necessarily unprecedented. Intramolecular hydrogen bonds in carbohydrates have been reported in other molecular mechanic and molecular dynamic studies [9,42,51,80] as well as in experimental studies [40,74]. The majority of these studies involve hydrogen bonds between adjacent residues. However, as determined from electron and X-ray diffraction studies, dextran is stabilized by hydrogen bonds

between the i and i+2 residues [40]. In the molecular dynamics simulation of a triantennary oligosaccharide model for an asialoglycoprotein receptor ligand, several hydrogen bonds were found between branches spanning as many as five contiguous residues [9].

The loop region of carbohydrate receptors in *S. oralis* strains 34 and J22 consist of three sugar residues while the *S. oralis* ATCC 55229 receptor has four. The difference in the size of the loops probably lies with the fact that the receptors for strains 34 and J22 have a Gal*fβ*(1→6)Gal*pβ* glycosidic linkage. This provides an extra degree of freedom with rotation about the C5–C6 bond thereby enabling the smaller loop to be formed [87].

There remain several aspects of the proposed adhesin recognition loop which remain unclear. The first is the structural role for the Gal*fβ* residue. The common residue appears to be considerably flexible in these simulations, consistent with other studies of furanose rings [70,71,89]. How the flexibility may affect the loop formation remains to be determined. Second, it is uncertain at this time if the Gal*fβ* ring is even required for closure of the loop. The hydrogen bonding interactions between the phosphate and the furanose ring are to one of the ring hydroxyl groups in all three models. In two of the models studied (*S. oralis* strains ATCC 55229 and J22), interactions were also found with the C5 hydroxyl group of the Gal*fβ*. No similar interaction was found in the *S. oralis* 34 model. It has been reported by Hardy and Sarko [42] that the strongest hydrogen bonds in a molecular dynamics simulation are to the pendant as opposed to ring hydroxyl groups. A similar phenomenon may be occurring in this study. Thus, it is unclear, if there are unique structural features within the Gal*fβ* ring required for interactions with the phosphate. Third, it is not obvious why the loop should form between the Gal*fβ* and the phosphate to the reducing end of the oligomer. In the course of each of the three molecular dynamics simulations, no interactions occurred between the Gal*fβ* and the phosphate residue at the non-reducing end. Further work is required to determine why Gal*fβ* would interact exclusively with the phosphate residue at the reducing end.

The theoretical nature of the modeling findings must be emphasized. From predictions of secondary structures such as these, experimental investigations, primarily by several solution NMR techniques [38,75], may be undertaken in order to test these models.

Conclusions

The human mouth contains a diversity of surfaces each within a different microenvironment, with every surface presenting a different challenge to a bacterium seeking to attach. These sites are continually bathed with host fluids containing proteins that attach to these surfaces, particularly to tooth surfaces. These adherent proteins, the acquired pellicle, provide new binding sites for bacteria utilizing adhesin proteins. Primary colonizing bacterial species, predominantly streptococci, adhere to the acquired pellicle, and again provide a new substratum for the next round of adherent bacteria. Primary colonizing species adhere to each other and secondary species adhere to the primary species, resulting in microbial ecological succession and biofilm formation. The properties of the surface dictate which proteins will adhere, and the properties of these adherent proteins will dictate which bacteria will then be able to attach. Ultimately the properties of the binding and receptor molecules drive what proteins and what bacteria will adhere. Continued investigations into the molecular nature of microbial adherence is adding to our understanding of protein-to-carbohydrate interactions, while enriching our appreciation of how oral ecological diversity may be a direct result of molecular structural diversity.

Acknowledgements

This research was supported in part by a research award from the Warner-Lambert Company to FJC. The authors thank Dr Herman van Halbeek (Complex Carbohydrate Research Center, University of Georgia) for invaluable collaboration, and Drs Charles E McQueen (Walter Reed Army Institute of Research, Washington, DC), Jack London and Paul Kolenbrander (National Institute of Dental Research, NIH, Bethesda, MD) for critically reading the manuscript and for their continued support and encouragement.

References

1 Abeygunawardana C and CA Bush. 1993. Determination of the chemical structure of complex polysaccharides by heteronuclear NMR spectroscopy. Adv Biophys Chem 3: 199–249.
2 Abeygunawardana C, CA Bush and JO Cisar. 1990. Complete structure of the polysaccharide from *Streptococcus sanguis* J22. Biochem 29: 234–248.
3 Abeygunawardana C, CA Bush and JO Cisar. 1991. Complete structure of the cell surface polysaccharide of *Streptococcus oralis* ATCC 10557: a receptor for lectin-mediated interbacterial adherence. Biochem 30: 6528–6540.
4 Abeygunawardana C, CA Bush and JO Cisar. 1991. Complete structure of the cell surface polysaccharide of *Streptococcus oralis* C104: a 600-MHz NMR study. Biochem 30: 8568–8577.
5 Amano A, HT Sojar, JY Lee, A Sharma, MJ Levine and RJ Genco. 1994. Salivary receptors for recombinant fimbrillin of *Porphyromonas gingivalis*. Infect Immun 62: 3372–3380.
6 Azen E, A Prakobphol and SJ Fisher. 1993. PRB3 null mutations result in absence of the proline-rich glycoprotein G1 and abolish *Fusobacterium nucleatum* interactions with saliva *in vitro*. Infect Immun 61: 4434–4439.
7 Babu JP, EH Beachey, DL Hasty and WA Simpson. 1986. Isolation and characterization of a 60-kilodalton salivary glycoprotein with agglutinating activity against strains of *Streptococcus mutans*. Infect Immun 56: 2484–2490.
8 Babu JP, MK Dabbous and SN Abraham. 1991. Isolation and characterization of a 180 kiloDalton salivary glycoprotein which mediates the attachment of *Actinomyces naeslundii* to human buccal epithelial cells. J Perio Res 26: 97–106.
9 Balaji PV, PK Qasba and VSR Rao. 1993. Molecular dynamics simulations of asialoglycoprotein receptor ligands. Biochem 32: 12599–12611.
10 Bennick A, AC McLaughlin, AA Grey and G Madapallimattam. 1981. The location and nature of calcium-binding sites in salivary acidic proline-rich phosphoproteins. J Biol Chem 256: 4741–4746.
11 Bergey EJ, MJ Levine, MS Reddy, SD Bradway and I Al-Hashimi. 1986. Use of the photoaffinity cross-linking agent *N*-hydroxysuccinimidyl-4-azidosalicylic acid to characterize salivary glycoprotein bacterial interactions. Biochem J 234: 43–48.
12 Brennan MJ, JO Cisar and AL Sandberg. 1986. A 160-kilodalton epithelial cell surface glycoprotein recognized by plant lectins that inhibit the adherence of *Actinomyces naeslundii*. Infect Immun 52: 840–845.

13 Brennan MJ, JO Cisar, AE Vatter and AL Sandberg. 1984. Lectin-dependent attachment of *Actinomyces naeslundii* to receptors on epithelial cells. Infect Immun 46: 459–464.
14 Brennan MJ, RA Joralmon, JO Cisar and AL Sandberg. 1987. Binding of *Actinomyces naeslundii* to glycosphingolipids. Infect Immun 55: 487–489.
15 Cassels FJ, HM Fales, J London, RW Carlson and H van Halbeek. 1990. Structure of a streptococcal adhesin carbohydrate receptor. J Biol Chem 265: 14127–14135.
16 Cassels FJ and J London. 1989. Isolation of a coaggregation-inhibiting cell wall polysaccharide from *Streptococcus sanguis* H1. J Bacteriol 171: 4019–4025.
17 Cassels FJ and H van Halbeek. 1995. Isolation and characterization of adhesin polysaccharide receptors. Meth Enzymol 252: 69–91.
18 Cisar JO. 1986. Fimbrial lectins of the oral Actinomyces. In: Microbial Lectins and Agglutinins (Mirelman D, ed), pp 183–196, John Wiley and Sons, New York.
19 Cisar JO, PE Kolenbrander and FC McIntire. 1979. Specificity of coaggregation reactions between human oral streptococci and strains of *Actinomyces viscosus* or *Actinomyces naeslundii*. Infect Immun 24: 742–752.
20 Cisar JO, AL Sandberg and SE Mergenhagen. 1984. The function and distribution of different fimbriae on strains of *Actinomyces viscosus* and *Actinomyces naeslundii*. J Dent Res 63: 393–396.
21 Clark WB, JE Beem, WE Nesbitt, JO Cisar, CC Tseng and MJ Levine. 1989. Pellicle receptors for *Actinomyces viscosus* type 1 fimbriae *in vitro*. Infect Immun 57: 3003–3008.
22 Clark WB, TT Wheeler, MD Lane and JO Cisar. 1986. *Actinomyces* adsorption mediated type 1 fimbriae. J Dent Res 65: 1166–1168.
23 Costello AH, JO Cisar, PE Kolenbrander and O Gabriel. 1979. Neuraminidase-dependent hemagglutination of human erythrocytes by human strains of *Actinomyces viscosus* and *Actinomyces naeslundii*. Infect Immun 26: 563–572.
24 Demuth DR, CA Davis, AM Corner, RJ Lamont, PS Leboy and PS Malamud. 1988. Cloning and expression of a *Streptococcus sanguis* surface antigen that interacts with a human salivary agglutinin. Infect Immun 56: 2484–2490.
25 Demuth DR, EE Golub and D Malamud. 1990. Streptococcal-host interactions. Structural and functional analysis of a *Streptococcus sanguis* receptor for a human salivary glycoprotein. J Biol Chem 265: 7120–7126.
26 Demuth DR, MS Lammey, M Huck, ET Lally and D Malamud. 1990. Comparison of *Streptococcus mutans* and *Streptococcus sanguis* receptors for human salivary agglutinin. Microb Pathogen 9: 199–211.
27 Douglas CW. 1983. The binding of human salivary α-amylase by oral strains of streptococcal bacteria. Arch Oral Biol 28: 567–573.
28 Drake D, KG Taylor, AS Bleiweis and RJ Doyle. 1988. Specificity of the glucan-binding lectin of *Streptococcus cretus*. Infect Immun 56: 1864–1872.
29 Edge CJ, UC Singh, R Bazzo, GL Taylor, RA Dwek and TW Rademacher. 1990. 500-picosecond molecular dynamics in water of the man-α1→2manα glycosidic linkage present in asn-linked oligomannose-type structures on glycoprotein. Biochem 29: 1971–1974.
30 Ericson T and J Rundegren. 1983. Characterization of a salivary agglutinin reacting with a serotype c strain of *Streptococcus mutans*. Eur J Biochem 133: 255–261.
31 Ganeshkumar N, PM Hannam, PE Kolenbrander and BC McBride. 1991. Nucleotide sequence of a gene coding for a saliva-binding protein (SsaB) from *Streptococcus sanguis* 12 and possible role of the protein in coaggregation with actinomyces. Infect Immun 59: 1093–1099.
32 Gibbons RF and DI Hay. 1988. Human salivary acidic proline-rich proteins and statherin promote the attachment of *Actinomyces viscosus* LY7 to apatitic surfaces. Infect Immun 56: 439–445.
33 Gibbons RJ, L Cohen and DI Hay. 1986. Strains of *Streptococcus mutans* and *Streptococcus sobrinus* attach to different pellicle receptors. Infect Immun 52: 555–561.
34 Gibbons RJ and DI Hay. 1989. Adsorbed salivary acidic proline-rich proteins contribute to the adhesion of *Streptococcus mutans* JBP to apatitic surfaces. J Dent Res 68: 1303–1307.
35 Gibbons RJ, DI Hay, JO Cisar and WB Clark. 1988. Adsorbed salivary proline-rich protein 1 and statherin: receptors for type 1 fimbriae of *Actinomyces viscosus* T14V on apatitic surfaces. Infect Immun 56: 2990–2993.
36 Gibbons RJ, DI Hay and DH Schlesinger, 1991. Delineation of a segment of adsorbed salivary acidic proline-rich proteins which promotes adhesion of *Streptococcus gordonii* to apatitic surfaces. Infect Immun 59: 2948–2954.
37 Gillece-Castro BL, A Prakobphol, AL Burlingame, H Leffler and SJ Fisher. 1991. Structure and bacterial receptor activity of a human salivary proline-rich glycoprotein. J Biol Chem 266: 17358–17368.
38 Gitti R, G Long and CA Bush. 1994. Measurement of long-range C^{13}-H^1 coupling constants of 95% uniformly labeled polysaccharide from *Streptococcus mitis* J22. Biopolymers 34: 1327–1338.
39 Glushka J, FJ Cassels, RW Carlson and H van Halbeek. 1992. Complete structure of the adhesin receptor polysaccharide of *Streptococcus oralis* ATCC 55229 (*Streptococcus sanguis* H1). Biochem 31: 10741–10746.
40 Guizard C, H Chanzy and A Sarko. 1984. Molecular and crystal structure of dextrans: a combined electron and x-ray diffraction study. 1. The anhydrous high-temperature polymorph. Macromolecules 17: 100–107.
41 Hardy BJ and A Sarko. 1993. Conformational analysis and molecular dynamics simulation of cellobiose and larger cellooligomers. J Comp Chem 14: 831–847.
42 Hardy BJ and A Sarko. 1993. Molecular dynamics simulation of cellobiose in water. J Comp Chem 14: 848–857.
43 Hawkins BW, RD Cannon and HF Jenkinson. 1993. Interactions of *Actinomyces naeslundii* strains T14V and ATCC 12104 with saliva, collagen and fibrinogen. Arch Oral Biol 38: 533–535.
44 Hay DI, A Bennick, DH Schlessinger, K Minaguchi, G Madapallimattam and SK Schlickebler. 1988. The primary structures of six human salivary acidic proline-rich proteins (PRP-1, PRP-2, PRP-3, PRP-4, PIF-s and PIF-f). Biochem J 255: 15–21.
45 Hiroi T, K Fukushima, I Kantake, Y Namiki and T Ikeda. 1992. *De novo* glucan synthesis by mutans streptococcal glycosyltransferases present in pellicle promotes firm binding of *Streptococcus gordonii* to tooth surfaces. FEMS Microbiol Lett 96: 193–198.
46 Homans SW. 1990. A molecular mechanical force field for the conformational analysis of oligosaccharides: comparison of theoretical and crystal structures of Manα1-3Manβ1-4GlcNAc. Biochem 29: 9110–9118.
47 Hsu SD, JO Cisar, AL Sandberg and M Kilian. 1994. Adhesive properties of viridians streptococcal species. Microb Ecol Health Dis 7: 125–137.
48 Kaufman J and JM DiRienzo. 1989. Isolation of a corncob (coaggregation) receptor polypeptide from *Fusobacterium nucleatum*. Infect Immun 57: 331–337.
49 Kishimoto E, DI Hay and RJ Gibbons. 1989. A human salivary protein promotes adhesion of *Streptococcus mutans* serotype c strains to hydroxyapatite. Infect Immun 57: 3702–3707.
50 Kishimoto E, DI Hay and R Kent. 1990. Polymorphism of submandibular-sublingual salivary proteins which promote adhesion of *Streptococcus mutans* serotype c strains to hydroxyapatite. J Dent Res 69: 1741–1745.
51 Koehler JEH, W Saenger and WF van Gunsteren. 1988. Conformational differences between α-cyclodextrin in aqueous solution and in crystalline form. J Mol Biol 203: 241–250.
52 Kolenbrander PE, N Ganeshkumar, FJ Cassels and CV Hughes. 1993. Coaggregation: specific adherence among human oral plaque bacteria. FASEB J 7: 406–413.
53 Kolenbrander PE and J London. 1993. Adhere today, here tomorrow: oral bacterial adherence. J Bacteriol 175: 3247–3252.
54 Kolenbrander PK and RN Andersen. 1990. Characterization of *Streptococcus gordonii (S. sanguis)* PK488 adhesin-mediated coaggregation with *Actinomyces naeslundii* PK606. Infect Immun 58: 3064–3072.
55 Kolenbrander PK and BL Williams. 1981. Lactose-reversible coaggregation between oral actinomycetes and *Streptococcus sanguis*. Infect Immun 26: 563–572.
56 Lantz MS, RD Allen, P Bounelis, LM Switalski and M Höök. 1990. *Bacteroides gingivalis* and *Bacteroides intermedius* recognize different sites on human fibrinogen. J Bacteriol 172: 716–726.
57 Lantz MS, RD Allen, LW Duck, JL Blume, LM Switalski and M Höök. 1991. Identification of *Porphyromonas gingivalis* components that mediate its interactions with fibronectin. J Bacteriol 173: 4263–4270.
58 Lantz MS, RD Allen, TA Vail, LM Switalski and M Höök. 1991.

Specific cell components of *Bacteroides gingivalis* mediate binding and degradation of human fibrinogen. J Bacteriol 173: 495–504.
59 Lantz MS, RW Rowland, LM Switalski and M Höök. 1986. Interactions of *Bacteroides gingivalis* with fibrinogen. Infect Immun 54: 656–658.
60 Lantz MS, LM Switalski, KS Kornman and M Höök. 1985. *Bacteroides intermedius* binds fibrinogen. J Bacteriol 163: 623–628.
61 Levine MJ, MC Herzberg, MS Levine, SA Ellison, MW Stinson, HC Li and T van Dyke. 1978. Specificity of salivary-bacterial interactions: role of terminal sialic acid residues in the interaction of salivary glycoproteins with *Streptococcus sanguis* and *Streptococcus mutans*. Infect Immun 19: 107–115.
62 Liu T, RJ Gibbons and DI Hay. 1990. *Streptococcus cricetus* and *Streptococcus rattus* bind to different segment of collagen molecules. Oral Micro Immun 5: 143–148.
63 Liu T, RJ Gibbons, DI Hay and Z Skobe. 1991. Binding of *Actinomyces viscosus* to collagen: association with the type 1 fimbrial adhesin. Oral Micro Immun 6: 1–5.
64 McIntire FC, CA Bush, SS Wu, SC Li, YT Li, M McNeil, S Tjoa and PV Fennessey. 1987. Structure of a new hexasaccharide of *Streptococcus sanguis* 34. Carbohydr Res 166: 133–143.
65 McIntire FC, LK Crosby, JJ Barlow and KL Matta. 1984. Structural preference of β-galactosides-reactive lectins on *Actinomyces viscosus* T14V and *Actinomyces viscosus* WVU45. Infect Immun 41: 848–850.
66 McIntire FC, LK Crosby, AE Vatter, JO Cisar, MR McNeil, CA Bush, SS Tjoa and PV Fennessey. 1988. A polysaccharide from *Streptococcus sanguis* 34 that inhibits coaggregation of *S. sanguis* 34 and *Actinomyces viscosus* T14V. J Bacteriol 170: 2229–2235.
67 Moreno EC, M Kresak and DI Hay. 1982. Adsorption thermodynamics of acidic proline-rich salivary proteins onto calcium apatites. J Biol Chem 257: 2981–2989.
68 Murray PA, A Prakobphol, T Lee, CI Hoover and SJ Fisher. 1992. Adherence of oral streptococci to salivary glycoproteins. Infect Immun 60: 31–38.
69 Nyvad B and M Kilian. 1978. Microbiology of the early colonization of human enamel and root surfaces *in vivo*. Scan J Dent Res 95: 369–380.
70 Olson WK. 1982. How flexible is the furanose ring? 2. An updated potential energy estimate. J Am Chem Soc 104: 278–286.
71 Olson WK and JL Sussman. 1982. How flexible is the furanose ring? 1. A comparison of experimental and theoretical studies. J Am Chem Soc 104: 270–278.
72 Oppenheim FG, DI Hay and C Franzblau. 1971. Proline-rich proteins from human parotid saliva. Isolation and partial characterization. Biochem 10: 4233–4238.
73 Oppenheim FG, GD Offer and RF Troxler. 1985. Amino acid sequence of a proline-rich phosphoglycoprotein from parotid secretion of the subhuman primate, *Macaca fascicularis*. J Biol Chem 260: 10671–10679.
74 Pérez S. 1991. Molecular modeling and electron diffraction of polysaccharides. Meth Enzymol 203: 510–556.
75 Poppe L, R Struike-Prill, B Meyer and H van Halbeek. 1992. The solution conformation of sialyl-α(2→6)-lactose studied by modern NMR techniques and Monte Carlo simulation. J Biomol NMR 2: 109–136.
76 Prakobphol A, H Leffler and SJ Fisher. 1995. Identifying bacterial receptor proteins and quantifying the strength of the interactions they mediate. Meth Enzymol 252: 132–142.
77 Prakobphol A, PA Murray and SJ Fisher. 1987. Bacterial adherence on replicas of sodium dodecyl sulfate-polyacrylamide gels. Anal Biochem 164: 5–11.
78 Reddy GP, C Abeygunawardana, CA Bush and JO Cisar. 1994. The cell wall polysaccharide of *Streptococcus gordonii* 38: structure and immunochemical comparison with the receptor polysaccharides of *Streptococcus oralis* 34 and *Streptococcus mitis* J22. Glycobiol 4: 183–192.
79 Reddy GP, CC Chang and CA Bush. 1993. Determination by heteronuclear NMR spectroscopy of the complete structure of the cell wall polysaccharide of *Streptococcus sanguis* strain K103. Anal Chem 65: 913–921.
80 Sathyanarayana BK and VSR Rao. 1971. Conformational studies of β-glucans. Biopolymers 10: 1605–1615.
81 Scannapieco FA, EJ Bergey, MS Reddy and MJ Levine. 1989. Characterization of salivary alpha-amylase binding to *Streptococcus sanguis*. Infect Immun 57: 2853–2863.
82 Schilling KM and WH Bowen. 1992. Glucans synthesized in situ in experimental pellicle function as specific binding sites for *Streptococcus mutans*. Infect Immun 60: 284–295.
83 Stinson MW, MJ Levine, JM Cavese, A Prakobphol, PA Murray, LA Tabak and MS Reddy. 1982. Adherence of *Streptotoccus sanguis* to salivary mucin bound to glass. J Dent Res 61: 1390–1393.
84 Strömberg N and T Borén. 1992. Actinomyces tissue specificity may depend on differences in receptor specificity for GalNAcβ-containing glycoconjugates. Infect Immun 60: 3268–3277.
85 Strömberg N and K-A Karlsson. 1990. Characterization of the binding of *Actinomyces naeslundii* (ATCC 12104) and *Actinomyces viscosus* (ATCC 19246) to glycosphingolipids using a solid-phase overlay approach. J Biol Chem 265: 11251–11258.
86 Strömberg N and K-A Karlsson. 1990. Characterization of the binding of *Propionibacterium granulosum* to glycosphingolipids adsorbed on surfaces. J Biol Chem 265: 11244–11250.
87 Stuike-Prill R and B Meyer. 1990. A new force-field program for the calculation of glycopeptides and its application to a heptacosapeptide-decasaccharide of immunoglobulin G_1: importance of 1-6-glycosidic linkages in carbohydrate-peptide interactions. Eur J Biochem 194: 903–919.
88 Switalski LM, WG Butcher, PC Caufield and MS Lantz. 1993. Collagen mediates adhesion of *Streptococcus mutans* to human dentin. Infect Immun 61: 4119–4125.
89 Van Eijck BP and J Kroon. 1989. Molecular-dynamics simulations of β-D-ribose and β-D-deoxyribose solutions. J Mol Struc 195: 133–146.
90 Weiner PK and PA Kollman. 1981. AMBER: assisted model building with energy refinement. A general program for modeling molecules and their interactions. J Comput Chem 2: 287–303.
91 Weiss EI, I Eli, B Shenitzki and N Smorodinsky. 1990. Identification of the rhamnose-sensitive adhesin of *Capnocytophaga ochracea* ATCC 33596. Arch Oral Biol 35: 127S–130S.
92 Weiss EI, J London, PE Kolenbrander, AS Kagermeier and RN Andersen. 1987. Characterization of lectinlike surface components on *Capnocytophaga ochracea* ATCC 33596 that mediate coaggregation with gram-positive oral bacteria. Infect Immun 55: 1198–1202.